^{1}H NMR Studies of λ Cro Repressor. 2. Sequential Resonance Assignments of the ^{1}H NMR Spectrum†

Paul L. Weber,‡ David E. Wemmer,§,‖ and Brian R. Reid*,‡,§

Departments of Biochemistry and Chemistry, University of Washington, Seattle, Washington 98195

Received March 27, 1985

ABSTRACT: The cro repressor protein from bacteriophage λ has been studied in solution by two-dimensional nuclear magnetic resonance spectroscopy (2D NMR). Following the approach of Wüthrich and co-workers [Wüthrich, K., Wider, G., Wagner, G., & Braun, W. (1982) *J. Mol. Biol. 155*, 311–319], individual spin systems were identified by *J*-correlated spectroscopy (COSY) supplemented, where necessary, by relayed coherence transfer spectroscopy (RELAY). Nuclear Overhauser effect spectroscopy (NOESY) was used to obtain sequence-specific assignments. From the two-dimensional spectra, the peptide backbone resonances (NH and $C^{\alpha}H$) for 65 of the 66 amino acids were assigned, as well as most of the side chain resonances. The chemical shifts for the assigned protons are reported at 35 °C in 10 mM potassium phosphate, pH 6.8, and in 10 mM potassium phosphate, pH 4.6, 0.2 M KCl, and 0.1 mM EDTA. Small shifts were observed for some resonances upon addition of salt, but no major changes in the spectrum were seen, indicating that no global structural change occurs between these ionic strengths. NOE patterns characteristic of α-helices, β-strands, and turns are seen in various regions of the primary sequence. From the location of these regions the secondary structure of cro in solution appears to be virtually identical with the crystal structure [Anderson, W. F., Ohlendorf, D. H., Takeda, Y., & Matthews, B. W. (1981) *Nature (London) 290*, 754–758]. Missing assignments include the Pro-59 resonances and the peripheral protons of the eight lysine, the three arginine, and three of the five isoleucine residues.

Cro repressor is a small protein (66 amino acids, M_r 7351) that binds to the right operator region (O_R) of bacteriophage λ as an essential component in the regulation of the lytic mode of phage development [for a review, see Ptashne et al. (1980)]. This system is an excellent example of sequence-specific recognition of DNA by a protein and, given the size of the intact repressor, is amenable to detailed physicochemical and structural investigation. The crystal structure of cro has been solved (Anderson et al., 1981); on the basis of these coordinates, a model for the interaction of cro with the O_R3 operator DNA sequence has been proposed (Ohlendorf et al., 1982). This model, however, lacks direct experimental support.

We are currently using nuclear magnetic resonance (NMR) to investigate the molecular basis of sequence-specific recognition of DNA by proteins. NMR is a powerful analytical method, capable of determining both structural and dynamical characteristics of macromolecules. Our goal is to directly determine the contact points between cro and O_R3 by means of intermolecular NOEs.[1] Before the complex can be analyzed and interpreted, however, the NMR resonances of the DNA and of the repressor must first be separately assigned[2] to particular protons on the macromolecules. With the advent of sequential assignment methods for proteins (Wüthrich et al., 1982; Billeter et al., 1982) and nucleic acids (Hare et al., 1983; Scheek et al., 1983), it should now be possible to assign virtually every resonance in the NMR spectrum to the corresponding protons on the macromolecule. This has already been accomplished for both the exchangeable and nonexchangeable protons of the O_R3 operator (Chou et al., 1983; Ulrich et al., 1983; Wemmer et al., 1984). Once this is complete, information such as NOE intensities, *J* couplings, and proton exchange rates can be used to determine interproton distances, or dihedral angles, or breathing rates of the macromolecule in question. Both the structure and dynamics of the entire macromolecule can, in principle, be determined from these measurements. A particularly elegant example is the *lac* repressor headpiece, which has been sequentially assigned, and a structure for which has been determined from NOE intensities (Zuiderweg et al., 1983; Zuiderweg et al., 1984; Kaptein et al., 1985).

Cro repressor has already been the subject of NMR studies by other groups; identifications of the aromatic ring spin systems and a few well-shifted peaks have been attempted (Kirpichnikov et al., 1982; Kurochkin & Kirpichnikov, 1982; Iwahashi et al., 1982; Arndt et al., 1983). In addition, attempts were made to deduce some sequence-specific assignments by

† Supported in part by U.S. Health Service National Research Award 2 T32 GM07270 from the National Institute of General Medical Sciences (to P.L.W.), instrumentation grants from the Murdock Foundation, and NIH Program Project Grant GM32681.

* Address correspondence to this author at the Department of Chemistry.

‡ Department of Biochemistry.

§ Department of Chemistry.

‖ Present address: Department of Chemistry, University of California, Berkeley.

[1] Abbreviations: RELAY, two-dimensional relayed coherence transfer NMR spectroscopy; COSY, two-dimensional *J*-correlated NMR spectroscopy; NOE, nuclear Overhauser effect; NOESY, two-dimensional NOE spectroscopy; FID, free induction decay; DSS, sodium 4,4-dimethyl-4-silapentane-1-sulfonate; EDTA, ethylenediaminetetraacetic acid.

[2] In this paper, we continue to use the convention where *identification* means that groups of resonances can be recognized as belonging to a certain amino acid *type*, e.g., Val, Ile, etc., without any sequence information. An *assignment*, on the other hand, is most specific and means that the resonances belong to a *particular* amino acid, e.g., Val-25, Met-12, etc. The preceding paper dealt with a method for *identifying* spin systems; this paper utilizes that information in order to generate sequence-specific *assignments*.

0006-2960/85/0424-4553$01.50/0

using the X-ray structure data. Unfortunately, several of the spin system identities and sequence-specific assignments are incorrect. We report herein the sequential assignments for cro.

Materials and Methods

Purification of cro repressor is described in the preceding paper in this issue (Weber et al., 1985). Samples were dissolved either in 10 mM potassium phosphate, pH 6.8 buffer or in 10 mM phosphate, pH 4.6 buffer containing 0.2 M KCl and 0.1 mM EDTA. For spectra obtained in H_2O, 10% (v/v) D_2O was added for an internal lock signal. Samples in D_2O were prepared by first dissolving the sample in 0.36 mL of the appropriate buffer; following lyophilization, the dry powder was redissolved in 0.50 mL of 99.996% D_2O (Stohler Isotope Chemicals). Lyophilization was repeated, and the sample was dissolved in 0.36 mL of 99.996% D_2O. Following centrifugation in an Eppendorf microfuge, the sample was transferred to an NMR tube for data collection. Cro was stored in solution at 4 °C or was lyophilized and stored at −20 °C for long-term storage.

For sequential assignments, two-dimensional COSY, RELAY, and NOESY experiments were performed; the NOESY experiments were recorded in the phase-sensitive mode by the method of States (States et al., 1982), while the COSY and RELAY experiments were obtained as absolute magnitude spectra (Aue et al., 1976; Bax & Drobny, 1985). The mixing times for RELAY experiments were determined by methods described in the preceding paper in this issue (Weber et al., 1985), and the mixing times for NOESY experiments were varied between 100 and 150 ms for different experiments. All two-dimensional spectra were collected as 300–400 t_1 experiments each with 2K data points, with the carrier placed on the water resonance. Pulse phases were cycled as previously described (States et al., 1982; Bax & Drobny, 1985). For samples dissolved in H_2O, the water signal was irradiated for 2.5 s prior to the experimental pulse sequence; the decoupler was gated off before signal acquisition in t_2. All spectra were obtained on a Bruker WM-500 spectrometer at 30–35 °C using quadrature detection.

The data in all experiments were transferred to a VAX 11/780 for transformation and processing using software developed by Dr. Dennis Hare. Since transformation and plotting of the data could be completed in about a half-hour, several different window functions could be tested to obtain the best possible data set. A given two-dimensional experiment usually transformed best, however, using similar window functions: COSY and RELAY experiments were multiplied by a 0° phase-shifted sine bell extending out to twice the number of t_1 experiments (viz., to point 600–800 for experiments with 300–400 t_1 values), with the maximum skewed toward the beginning of the FID to compensate for relaxation. NOESY experiments usually were multiplied by a 60° (in D_2O) or 0° (in H_2O) phase-shifted sine bell, similarly skewed. Phase corrections were determined interactively prior to transformation. The 0° phase shift of the phase-sensitive NOESY spectrum in H_2O caused some problems in observing peaks near the diagonal (see discussion below) but yielded the best overall transformed spectrum. After transformation, the t_1 streaking was reduced when necessary by using the method of Klevit (1985).

Sequential resonance assignments were obtained by using the methods first proposed by Wüthrich and co-workers (Wüthrich et al., 1982; Billeter et al., 1982). In this method, the spin systems of individual amino acids are identified with a particular amino acid type. Next, backbone protons are connected using NOEs; these occur most often between nearest neighbors in the primary sequence. Sequence-specific information is then obtained by comparing unique peptide sequences in the observed connectivities with the known amino acid sequence of cro (Hsiang et al., 1977). Our approach differed slightly from this method, in that the side chain spin systems of almost half the residues could not initially be identified unambiguously; identification required first finding the backbone and (in some cases) $C^{\beta}H$ resonances using the sequential connectivities. Further side chain identification and assignment, when necessary, used the COSY, RELAY, and NOESY experiments. Efforts were made whenever possible to "overassign" each residue to increase the overall reliability of the assignments.

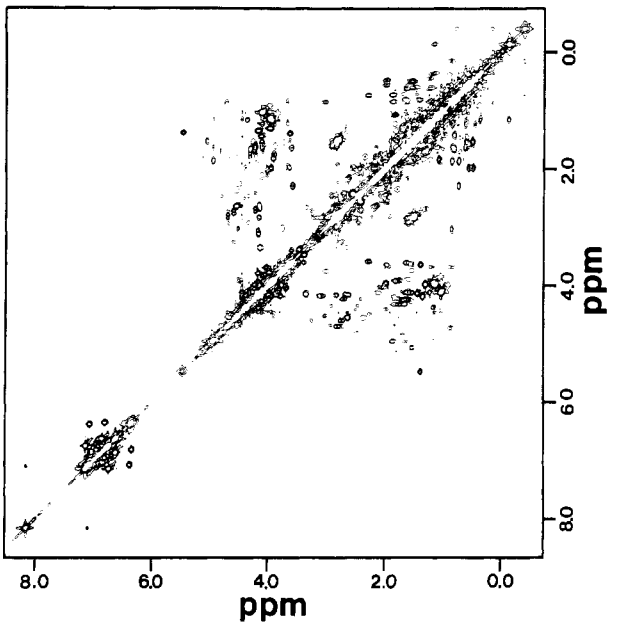

FIGURE 1: 500-MHz COSY absolute magnitude spectrum of cro repressor in 10 mM potassium phosphate, pH 6.8, in 99.996% D_2O. A spectral width of 5208 Hz was used, collecting 350 t_1 experiments, each in 2048 points. The final spctrum contains 1024 × 1024 points, for a digital resolution of 5.08 Hz/point.

A further obstacle in the assignments was the less than desirable NMR characteristics of cro repressor. The most recurrent problem was that the protein would gel at concentrations between 5 and 10 mM (monomer); hence spectra were obtained at relatively low concentrations for NMR work (1–3 mM). Furthermore, we were unable to observe amide resonances from cro freshly dissolved in D_2O (pH 4.6, 30 °C). Most likely this stems from the relatively low melting temperature of cro (Iwahashi et al., 1982) and from the fact that we cannot work at low pH, where amide exchange is slower (cro denatures at pH ≤4.6; Kurochkin & Kirpichinkov, 1982). Finally, reasonable spectra could only be obtained in the narrow temperature range 25–40 °C, with the best spectra consistently obtained at 30–35 °C. Above 35 °C, cro begins to denature; below 25 °C the line widths broaden significantly.

Results

Assignment of the Side Chain Spin Systems. COSY, RELAY, and NOESY spectra obtained in D_2O were used to unambiguously identify as many of the side chain spin systems as possible. Figure 1 shows the COSY spectrum used for identifying many of the side chain spin systems; subsequent figures (Figures 2–4) show expanded regions of these data. In addition, a RELAY experiment was designed to selectively optimize for valine, isoleucine, and threonine $C^{\alpha}H$–$C^{\gamma}H_3$ side

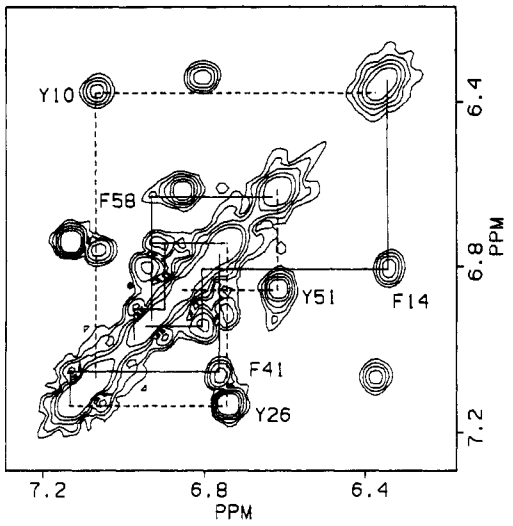

FIGURE 2: Identification of the aromatic ring spin systems in cro. The aromatic region of the COSY spectrum shown in Figure 1 is presented. Tyrosine rings are connected with a dashed line and phenylalanine rings by a solid line. The His-35 aromatic protons are not shown in this figure.

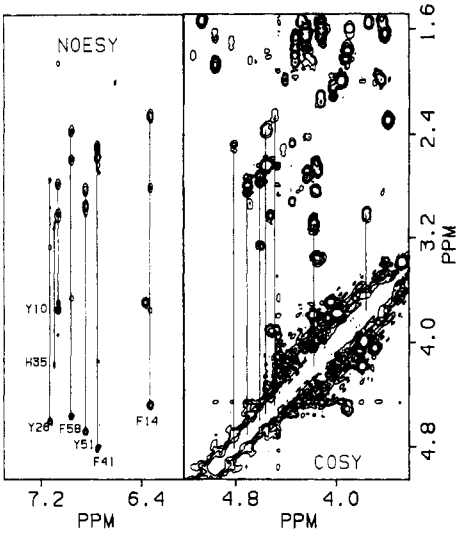

FIGURE 3: Attachment of the aromatic ring spin systems to the side chain $C^\alpha H$ and $C^\beta H$ resonances. The C^δ proton of each ring is close enough to the C^α and at least one of the C^β protons for an NOE to be observed. Left: NOESY in D_2O showing the NOEs from the ring protons to the C^α and C^β protons. The NOEs between the C^δ and C^α protons are labeled for each residue. Right: COSY in D_2O showing the corresponding $C^\alpha H$–$C^\beta H$ cross peaks. The mixing time of the NOESY experiment was 100 ms.

chain relays (see the preceding paper in this issue). With the six threonine side chains identified from the RELAY experiment, the eight alanines could be identified on the criteria of chemical shift and their distinctively strong $C^\alpha H$–$C^\beta H_3$ COSY cross peaks. Five of the alanines are well separated; three more are close in chemical shift near 4.00 ($C^\alpha H$) and 1.22 ppm ($C^\beta H_3$). Some resolution in these three peaks could be seen in the phase-sensitive NOESY, but not in the absolute magnitude COSY spectrum.

The aromatic residues in cro are three tyrosines, three phenylalanines, and one histidine. The aromatic ring spin systems were readily identified by using the COSY spectrum (Figure 2), and the NOESY spectrum was used to attach the rings to their α and β side chain protons (Figure 3) All three tyrosines and two of the three phenylalanines are reasonably well resolved in the COSY, as is the single histidine residue. The chemical shifts of the Tyr-10 $C^\delta H$ and the Phe-41 $C^\epsilon H$ resonances are the same (7.08 ppm), which made it difficult at first to connect the Phe-41 $C^\zeta H$ resonance to the proper COSY cross peak. The $C^\delta H$ and $C^\epsilon H$ resonances of each ring could be identified by intraresidue NOEs from the $C^\delta H$ to the side chain $C^\alpha H$ and $C^\beta H$ resonances, but it was not obvious which of the two rings was the phenylalanine. Once the $C^\alpha H$ and $C^\beta H$ resonances were sequentially assigned, the problem was trivial, and the $C^\zeta H$ resonance at 7.13 ppm was connected to the rest of the Phe-41 ring. One phenylalanine ring was more difficult than the others to identify, since it apparently flips at a slow rate relative to the NMR time scale (an alternative explanation of this finding is discussed below), resulting in a separate resonance for each of the five protons on the ring. The connectivity of this phenylalanine was determined and assigned to Phe-58 once the other aromatic protons were identified.

Only a few of the remaining side chain spin systems were identified prior to starting the sequential assignments; most side chain connectivities were determined during the sequential assignments or by elimination once the assignments had proceeded far enough. The $C^\alpha H$–$C^\beta H$ COSY cross peaks are identified in Figure 4, as determined directly from the COSY spectrum or by sequential assignments. The $C^\alpha H$–$C^\beta H_3$ COSY cross peak for Ala-11 was identified by elimination, once all of the threonine and the other seven alanine cross peaks were assigned. The two $C^\alpha H$–$C^\beta H$ cross peaks assigned to Arg-13 in Figure 4 are tentative; it is possible, but less likely, that these cross peaks are from the C^α and C^β protons of Pro-59.

Sequential Assignments of the Backbone Protons and Further Side Chain Identifications. The various types of sequential connectivities used in assigning protein spectra are shown in Figure 5. One or more of the through-space connections $d_{\alpha N}$, d_{NN}, and $d_{\beta N}$ will be short enough (<3.5 Å) for a NOE to occur. The validity of the sequential method is based upon the high probability that at least one of these NOEs is seen between nearest neighbors in the primary sequence (Billeter et al., 1982).[3] In addition, the type of sequential connectivity is usually indicative of the secondary structure present; stretches of $d_{\alpha N}$ NOEs occur in β-strands, while stretches of d_{NN} and $d_{\beta N}$ NOEs are found in α-helical regions. In helical residues additional connectivities between residues i and $i + 3$ are possible; the examples of $d_{\alpha_i N_{i+3}}$ and $d_{\alpha_i \beta_{i+3}}$ are also illustrated, but are not considered extensively in this paper. The cro spectrum has been assigned by use of only the $d_{\alpha N}$, d_{NN}, and $d_{\beta N}$ connectivities. Figures 6 and 7 summarize the residues connected sequentially by use of the $d_{\alpha N}$ connectivity. Four regions have been connected: from the C-terminal Ala-66 to Lys-62, from Phe-58 to Ser-49, from Asp-47 to Lys-39 (with a break between Thr-43 and Ile-44), and from Ile-5 to Met-1. Figure 8 shows the residues connected by use of d_{NN} NOEs. Here three segments were followed: from Leu-7 to Gly-15, from Lys-18 to Leu-23, and from Gln-27 to Arg-38. In addition, a short stretch was found between Ala-46 and Gly-48. Most residues connected by a d_{NN} NOE were also assigned by use of a $d_{\beta N}$ connectivity. All of these connectivities are discussed in more detail below.

(*i*) *Sequential Assignment of Residues in Extended Strands by $d_{\alpha N}$ NOEs.* The connectivity from Lys-62 to Ala-66 was easily identified since it contains the only Thr-Thr dipeptide in the protein. The Lys-62 and Lys-63 residues exhibit sharp,

[3] N.B. These designations have been changed from the original nomenclature of d_1, d_2, and d_3, respectively; see Stassinopoulou et al. (1984) and Wüthrich et al. (1984).

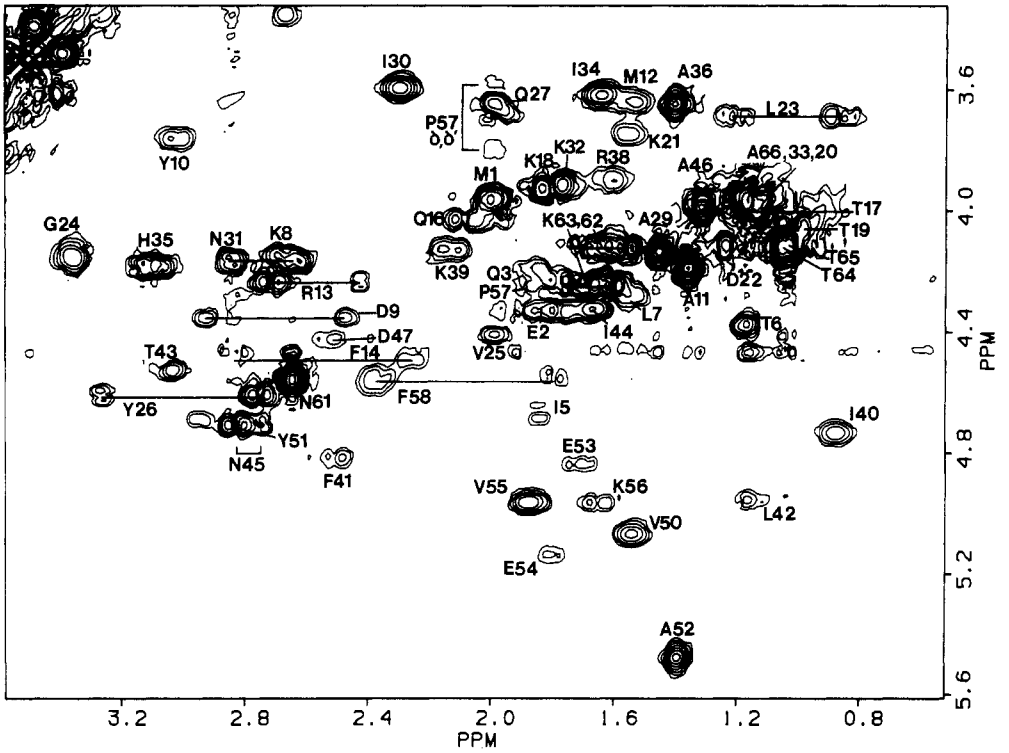

FIGURE 4: Sequence-specific identification of the $C^{\alpha}H$–$C^{\beta}H$ COSY cross peaks. An expansion of Figure 1 showing the region containing the $C^{\alpha}H$–$C^{\beta}H$ cross peaks for all residues except most threonines, serines and glycines. Additional cross peaks occur in this region for threonine $C^{\beta}H$–$C^{\gamma}H_3$ and proline $C^{\gamma}H_2$–$C^{\delta}H_2$ resonances. All cross peaks are sequentially identified.

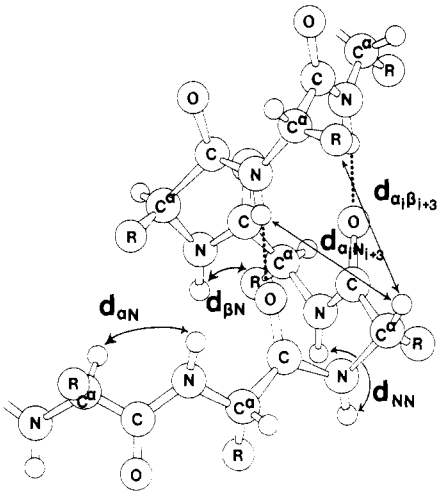

FIGURE 5: Nearest-neighbor connectivities that are used in sequentially assigning protein spectra. Arrows connect two protons that are nearby in space and give NOEs used in the sequential connectivities. The additional connectivities $d_{\alpha_iN_{i+3}}$ and $d_{\alpha_i\beta_{i+3}}$ for helical residues are also shown.

distinctive patterns of couplings in the $C^{\alpha}H$–$C^{\beta}H$ COSY cross peaks (apparent even in the absolute magnitude COSY spectrum), and the Thr-64, Thr-65, and Ala-66 resonances are also very sharp. We interpret these narrow line widths to be due to greater flexibility in this region; the extra motional freedom results in a shorter effective correlation time and consequently narrower resonances for these residues. The remaining resonances of the lysine side chains could not be unambiguously identified, due to the limited resolution in the relevant spectral regions.

The sequential connectivities for the backbone protons in the segment from Ser-49 through to Phe-58 were also clear and could be positioned in the primary sequence since the Val-50, Ala-52, and Val-55 side chains had been previously identified (without sequence information) by use of the RELAY experiment described earlier. The side chain of Tyr-51 was also previously identified, and since a Val-Tyr-Ala sequence occurs only once in the primary sequence, the positioning of this segment in the sequence was unambiguous. The side chain for Ser-49 was found by use of a weak $d_{\beta N}$ connection from Val-50. The identification of the Glu-53 and Glu-54 side chain resonances was made once their NH and $C^{\alpha}H$ resonances were found; Glu-54 is well resolved, and the $C^{\beta}H_2$ and $C^{\gamma}H_2$ resonances were previously identified in the COSY spectrum. The Glu-53 side chain could be assigned despite the overlap of the $C^{\alpha}H$ resonance of this residue and that of Phe-41. The position of the Lys-56 amide resonance was clear from the $d_{\alpha N}$ connectivity to Val-55, but the chemical shifts of the $C^{\alpha}H$ resonances for both of these residues and that of Leu-42 are, unforunately, all identical. Since the $C^{\beta}H$ resonances for Val-55 and Leu-42 had been previously assigned, the $C^{\beta}H_2$ resonance for Lys-56 could be assigned by elimination. The remaining Lys-56 side chain resonances were not found, again due to spectral crowding. The $C^{\alpha}H$ resonance of Lys-56 also gives a $d_{\alpha N}$-like connectivity to Pro-57, although in this case the connection is to the $C^{\delta}H_2$ resonances rather than to an amide proton. The rest of the proline side chain was then identified in the COSY and NOESY spectra obtained in D_2O. The connectivity ends at the amide of Phe-58, which gives a moderately strong NOE to the Pro-57 α proton (connection not shown in Figure 7).

In the next strand (residues Lys-39–Asp-47) a break occurred between Thr-43 and Ile-44, due to the loss of most of the Thr-43 $C^{\alpha}H$ signal from overlap with the irradiated solvent signal. In this strand the side chains for Ile-40, Thr-43, Ile-44, and Ala-46 were identified by the RELAY experiment. The spin systems for Asp-47 and Asn-45 were found once the amide and $C^{\alpha}H$ resonances were assigned; in addition, the side chain amide protons of Asn-45 were connected by NOEs to the $C^{\beta}H_2$ resonances (see Figure 9). And again, only the $C^{\beta}H_2$ reso-

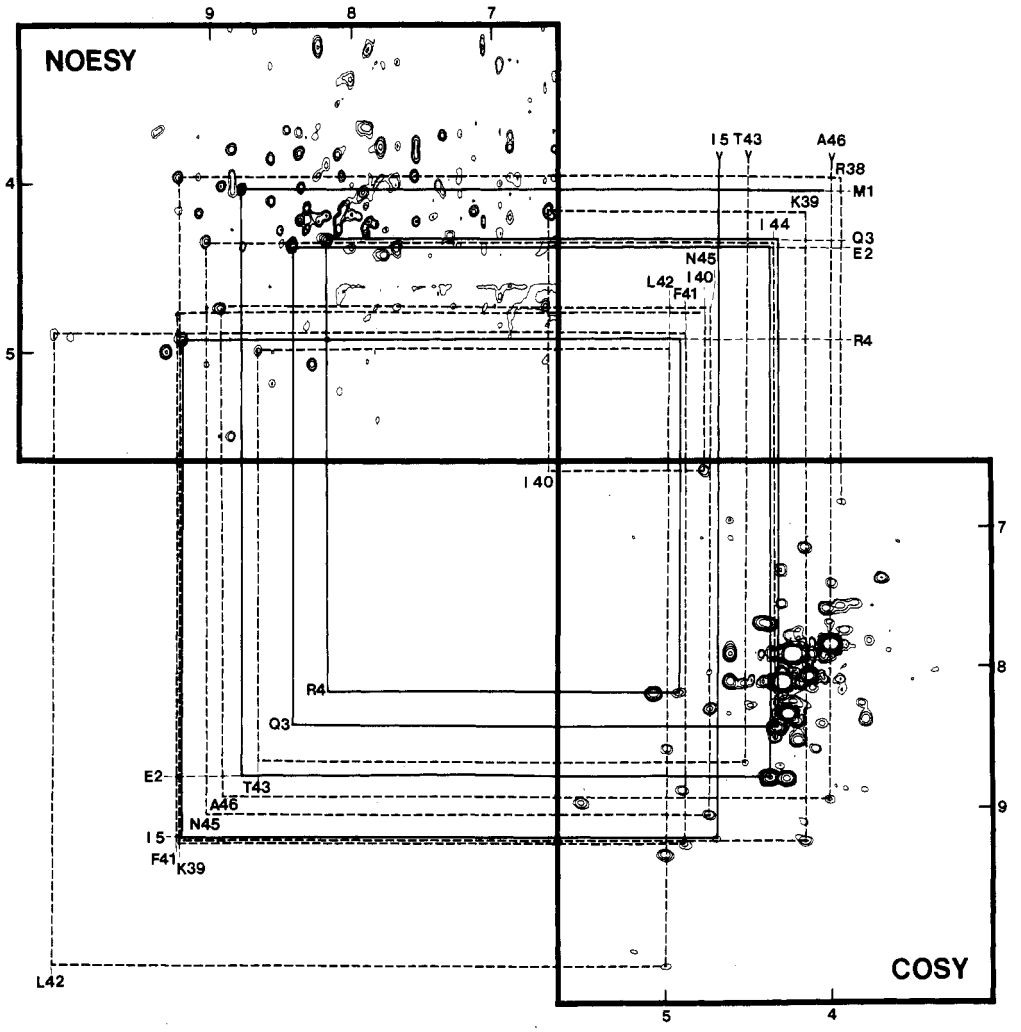

FIGURE 6: $d_{\alpha N}$ connectivities in cro. The region containing all of the NH–C$^\alpha$H cross peaks is plotted for NOESY andd COSY experiments performed on the same cro sample. Two extended strands are connected: residues M1–I5 (solid line) and residues R38–A46 (dashed line), with a break occurring between T43 and I44. The connectivities begin at the C-terminal residues (arrow heads) of the strands and end in the COSY plot (except for Met-1). Upper right: C$^\alpha$H resonances for residues connected by a solid line are to the right; for residues connected by dashed lines they are labeled above. Lower left: NH resonances for residues connected by solid lines are to the left; for residues connected by dashed lines they are labeled below. Some lines have been shifted slightly for clarity. The mixing time for the NOESY experiment was 150 ms.

nance of Lys-39 could be identified.

Following the assignment of the Ile-30 and Ile-34 resonances in the helical regions (see below), Ile-5 could be assigned by elimination. The sequence from Ile-5 through to Met-1 could be connected by use of $d_{\alpha N}$ NOEs, and the side chain spin systems for Met-1, Glu-2, Gln-3, and Arg-4 were identified once their C$^\alpha$H resonances were assigned. Their assignment was made clearer once overlapping resonances were eliminated (by sequentially assigning them to other spin systems). No NH_3–C$^\alpha$H COSY cross peak is seen for Met-1 due to exchange of the amino terminus with solvent. A $d_{\alpha N}$ NOE from Glu-2 is seen to the C$^\alpha$H resonances of Met-1, and its side chain can then be assigned. The COSY and RELAY cross peaks of the Met-1 side chains appear to be relatively strong; this may be due to some additional mobility of the amino terminus.

(ii) Sequential Assignment of Helical Residues by d_{NN} and $d_{\beta N}$ NOEs. Long stretches of amide–amide NOEs are indicative of α-helices, and three substantial segments with d_{NN} connectivities were found; one included the His-35 residue, the only unique amino acid in the protein. The complete His-35 spin system was easily found, in part since the C$^{\delta 2}$H and C$^{\epsilon 1}$H resonances were easily distinguished in the COSY spectrum. In the NOESY spectra, the cross peaks from the C$^{\delta 2}$H to C$^\alpha$H and C$^\beta$H could be recognized by the unusually narrow width of the aromatic resonance. From His-35, $d_{\beta N}$ and d_{NN} connectivities were made up to Arg-38 in one direction and back to Gln-27 in the other direction. No d_{NN} NOEs were seen between Ala-29 and Ile-30 or between Asn-31 and Lys-32, due to the closeness in chemical shift of the amide resonances involved. In both cases, the $d_{\beta N}$ NOEs were clear, and all side chain protons except for Ile-30, Lys-32, and Ile-34 could be completely identified. The amide side chain resonances for Gln-27 and Asn-31 could also be identified by NOEs from amides to their C$^\gamma$H$_2$ or C$^\beta$H$_2$ resonances, respectively (see Figure 9). The side chain of Ser-28 was also identified by $d_{\beta N}$ NOEs to the amide of Ala-29. In addition, several $d_{\alpha_i N_{i+3}}$ and $d_{\alpha_i \beta_{i+3}}$ connectivities in this helix could be made, supporting the sequential assignments.

The second stretch of d_{NN} and $d_{\beta N}$ connectivites occurs in the sequence between Leu-23 and Thr-17. In the data set shown in Figure 8, the Thr-17–Lys-18 d_{NN} NOE cannot be seen, but it is observable when the data are processed by using an 80° phase shift in the sine bell apodization function (not shown). The connectivities from Lys-18 through to Leu-23 are clear, and the previous identification of the Thr-19, Ala-20, and Leu-23 side chains helped in assigning this region. Once the NH and C$^\beta$H resonances were found (using the sequential

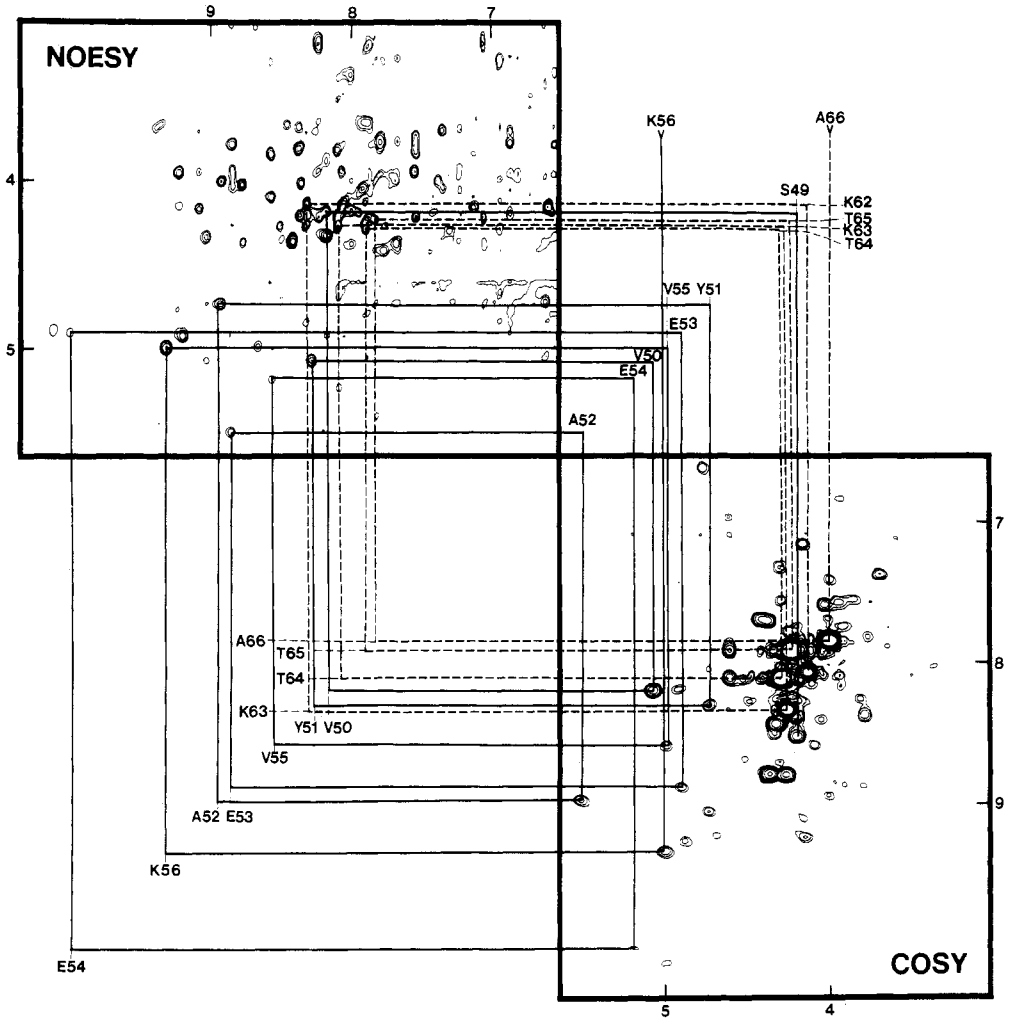

FIGURE 7: $d_{\alpha N}$ connectivities in cro. The same regions shown in Figure 6 are plotted. Two extended strands are connected: residues S49–K56 (solid line) and residues K62–A66 (dashed line). The connectivities begin at the C-terminal residues (arrow heads) of the strands and end in the COSY plot. Upper right: $C^{\alpha}H$ resonances for residues connected by a solid line are to the right; for residues connected by dashed lines they are labeled above. Lower left: NH resonances for residues connected by solid lines are to the left; for residues connected by dashed lines they are labeled below. Some lines have been shifted slightly for clarity.

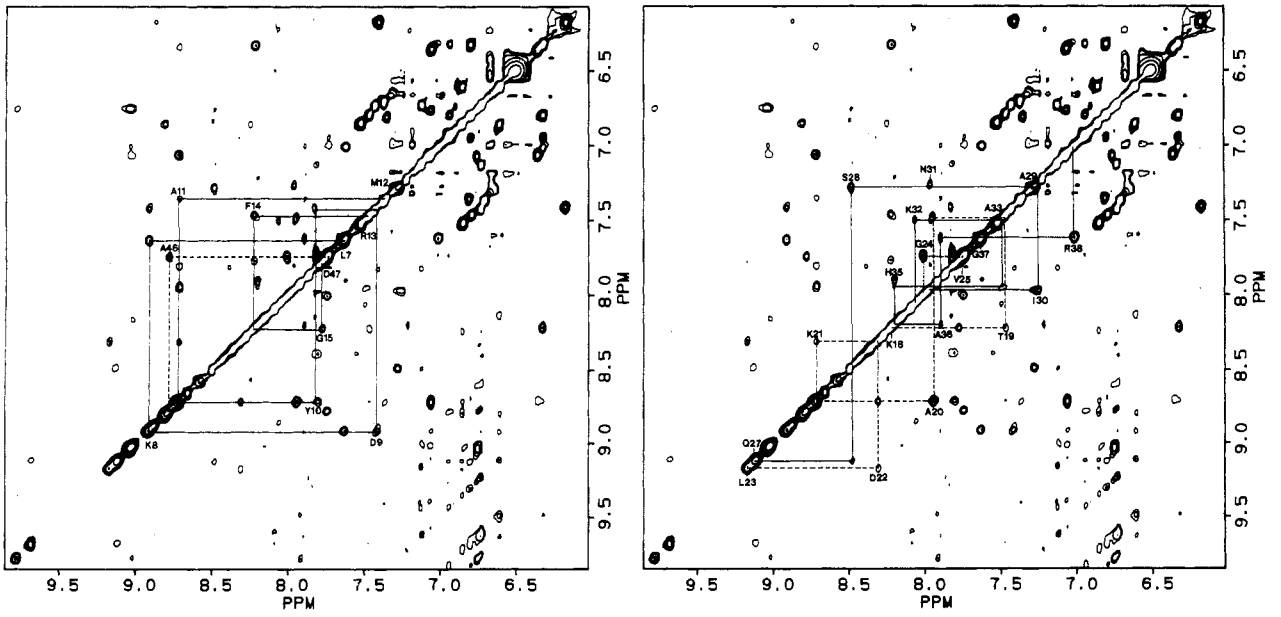

FIGURE 8: d_{NN} connectivities in cro. The same region is plotted in both the left- and right-hand figures. Most of the amide resonances have been labeled either directly above or directly below the corresponding peak. Left: d_{NN} connectivities for residues L7–G15; no NOE is seen between R13 and F14, due to the apodization. Also drawn (dashed line) is the connectivity from A46 to G48; the G48 amide resonance is not labeled, for clarity. Right: d_{NN} connectivities for residues K18–L23 (dashed line), G24–V25 (dashed-dotted line), and Q27–R38 (solid line). No NOEs are seen between T17 and K18, S28 and A29, and N31 and K32 due to the apodization used (see text).

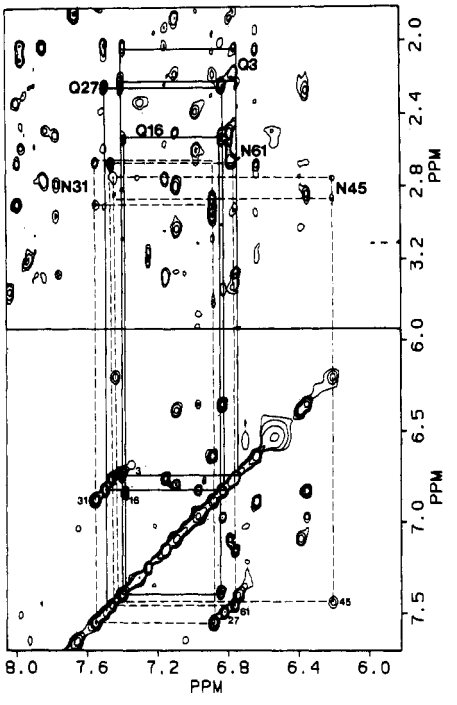

FIGURE 9: Identification of side chain amide resonances. NOESY diagram showing the connections of the side chain amide resonances to the asparagine $C^{\beta}H_2$ resonances (dashed lines) or glutamine $C^{\gamma}H_2$ resonances (solid lines). The mixing time for the NOESY was 150 ms.

connectivities), the corresponding $C^{\alpha}H$ resonances were easily determined. The Lys-18 and Lys-21 side chains could not be identified beyond the $C^{\beta}H$ resonances.

The third stretch of d_{NN} and $d_{\beta N}$ connectivities was found from Leu-7 to Gly-15, which includes the Tyr-10 and Phe-14 residues. After making the assignments described above, Tyr-10 could be assigned by elimination. In this stretch the Arg-13–Phe-14 d_{NN} NOE is missing, but the $d_{\beta N}$ NOE is seen. This again may be due to the harsh apodization of the NOESY spectrum. This stretch of helix is the weakest point in the assignments, as the NH–$C^{\alpha}H$ COSY cross peaks for Ala-11, Met-12, and Arg-13 have not been found. This is disturbing, but the d_{NN} NOEs are clear, and the sequential backbone NOEs can be connected from Leu-7 through Tyr-10, Ala-11, and Phe-14, all of whose side chains can be unambiguously identified.

(*iii*) *Assignment of the Remaining Residues.* The remaining unassigned residues, located between five of the six extended connectivities described above, were assigned either by short sequential connectivities or by elimination once all but one of a particular amino acid type had been assigned (Table I). The unassigned residues remaining at this point are Thr-6, Gln-16, Gly-24, Val-25, Tyr-26, Gly-48, Pro-59, Ser-60, and Asn-61. No sequential connectivities were observed for Thr-6, but it could be assigned by elimination (the NH–$C^{\alpha}H$ COSY cross peak is weak and not well resolved from the Lys-39 cross peak). Gln-16 can also be assigned by elimination, as it could be identified by the $\beta_2\gamma_2$ side chain; identification of the corresponding NH–$C^{\alpha}H$ COSY cross peak is straightforward.

A d_{NN} connectivity links Gly-24 with Val-25 and is extended by $d_{\alpha N}$ and $d_{\beta N}$ NOEs to Tyr-26. In one of the NOESY data sets collected a $d_{\alpha N}$ NOE from Tyr-26 to Gln-27 is observed, but is absent from Figures 6 and 7 due to the overlap of the Tyr-26 $C^{\alpha}H$ resonance with the solvent resonance. No connectivities could be made between Leu-23 and Gly-24, but the overall sequential assignments are not dependent upon this connection. The assignment of Gly-48 is made by connecting it to Asp-47 and then to Ala-46 in a short stretch of d_{NN} and $d_{\beta N}$ connectivities and by connecting it to Ser-49 by a weak d_{NN} NOE. Finally, both Ser-60 and Asn-61 can be assigned by elimination. The COSY cross peaks for these residues are sharper than most others in the COSY spectrum; most likely these residues are more flexible, as are residues 62–66. Pro-59 is the only unassigned amino acid remaining in cro, but no resonance assignments were possible since its COSY cross peaks are not observed. This is discussed in more detail below. Other assignments that are missing include all of the peripheral side chains of the eight lysine and three arginine residues, the $-SCH_3$ resonances of the two methionines (which could be identified but not *sequentially* assigned), and the C^{γ_1} and $C^{\delta}H_3$ resonances for isoleucines-5, -30, and -34.

Figure 10 summarizes the sequential NOE connectivities in cro. Some NOE connectivities that were observed but were weak or ambiguous have not been included in this figure. In addition, several $d_{\alpha_i\beta_{i+3}}$ and $d_{\alpha_iN_{i+3}}$ NOEs were seen in the helical regions but are not included since they only support what can already be concluded from the sequential assignment method. Figure 11 shows the COSY NH–$C^{\alpha}H$ "fingerprint" region for samples with and without 0.2 M KCl. The identity of the cross peak above the Glu-2 cross peak is unknown; it could arise from the splitting of some resonance due to an alternate

FIGURE 10: Summary of sequential connectivities in cro. Open bars represent weak NOE connectivities and closed bars strong NOE connectivities. Open circles denote those residues whose assignments depended upon elimination after assigning all remaining residues of that particular type. The "$d_{\alpha N}$" connectivity between Lys-56 and Pro-57 is actually between the $C^{\alpha}H$ resonance of Lys-56 and the $C^{\delta}H,H'$ resonances of Pro-57.

Table I: Sequence-Specific Resonance Assignments of the λ Cro Repressor ^{1}H NMR Spectrum[a]

residue	NH	$C^\alpha H$	$C^\beta H$	other	residue	NH	$C^\alpha H$	$C^\beta H$	other
Met-1	n.o.[b]	4.02	2.00, 2.00	$C^\gamma H_2$ 2.43, 2.43	Ala-33	7.51	4.00	1.12	
Glu-2	8.67	4.36	1.82, 1.92	$C^\gamma H_2$ 2.11, 2.03	Ile-34	7.94	3.64	1.65	$C^{\gamma 2}H_3$ 0.65
Gln-3	8.38	4.32	1.85, 1.99	$C^\gamma H_2$ 2.21, 2.03, $N^{\epsilon 2}H_2$ 7.39, 6.37	His-35	8.22	4.22	3.07, 3.12	$C^{\delta 2}H$ 7.24, $C^\epsilon H$ 8.15
					Ala-36	7.91	3.66	1.42	
Arg-4	8.17	4.90	1.47, 1.47	$C^\gamma H_2$ 1.55, 1.55	Gly-37	7.65	3.71, 3.92		
Ile-5	9.03	4.68	1.85	$C^{\gamma 2}H_3$ 1.10	Arg-38	7.03	3.94	1.60	
Thr-6	9.02	4.15	4.42	$C^{\gamma 2}H_3$ 1.22	Lys-39	9.05	4.14	2.17, 2.17	
Leu-7	7.64	4.29	1.55, 1.55	$C^\gamma H$ 1.57, $C^{\delta 1,2}H$ 0.57, 0.58	Ile-40	6.85	4.76	0.88	$C^{\gamma 2}H_3$ 0.17, $C^{\gamma 1}H_2$ 0.17, 0.82, $C^\delta H_3$ −0.39
Lys-8	8.93	4.16	2.70, 2.70		Phe-41	9.07	4.87	2.49, 2.49	$C^{\delta 1,2}H$ 6.78, 6.78, $C^{\epsilon 1,2}H$ 7.08, 7.08, $C^\zeta H$ 7.13
Asp-9	7.43	4.28	2.72, 2.43						
Tyr-10	7.85	3.77	3.03, 2.80	$C^{\delta 1,2}H$ 7.08, 7.08, $C^{\epsilon 1,2}H$ 6.38, 6.38	Leu-42	9.79	4.98	1.18, 1.18	$C^\gamma H$ 1.18, $C^{\delta 1,2}H_3$ 0.39, −0.12
					Thr-43	8.59	4.51	3.03	$C^{\gamma 2}H_3$ 0.87
Ala-11	8.74	4.24	1.41		Ile-44	8.44	4.33	1.68	$C^{\gamma 2}H_3$ 0.84
Met-12	7.38	3.69	1.56, 1.56		Asn-45	8.89, 8.83	4.72	2.86, 2.76	$N^{\delta 2}H_2$ 6.20, 7.43
Arg-13	7.48	4.26	2.74, 2.41		Ala-46	8.80, 8.73	4.00	1.34	
Phe-14	8.24	4.48	2.26, 2.84	$C^\gamma H_2$ 6.35, 6.35, $C^\epsilon H_2$ 6.82, 6.82, $C^\zeta H$ 6.96	Asp-47	7.76, 7.71	4.36	2.95, 2.50	
					Gly-48	7.82, 7.96	4.72, 4.72[c]		
Gly-15	7.79	4.30, 3.95			Ser-49	8.45, 8.37	4.19	3.80, 3.73	
Gln-16	7.67	4.05	2.10, 2.04	$C^\gamma H_2$ 2.44, 2.53, $N^{\epsilon 2}H_2$ 7.38, 6.82	Val-50	8.18	5.05	1.54	$C^{\gamma 1,2}H_3$ 0.52, 0.63
					Tyr-51	8.27	4.72	2.87, 2.95	$C^{\gamma 1,2}H$ 6.88, 6.88, $C^{\epsilon 1,2}H$ 6.63, 6.63
Thr-17	8.32	3.79	4.00	$C^{\gamma 2}H_3$ 1.15					
Lys-18	8.25	3.94	1.80, 1.80		Ala-52	8.81	5.48	1.41	
Thr-19	7.49	3.70	4.06	$C^{\gamma 2}H_3$ 0.90	Glu-53	8.75	4.89	1.68, 1.76	$C^\gamma H_2$ 2.01, 1.96
Ala-20	7.97	4.05	1.22		Glu-54	9.69	5.18	1.82, 1.82	$C^\gamma H_2$ 1.99, 1.99
Lys-21	8.74	3.78	1.64, 1.74		Val-55	8.50	4.98	1.88	$C^{\gamma 1,2}H_3$ 0.87, 0.76
Asp-22	8.34	4.20	1.35, 1.35		Lys-56	9.13	4.98	1.19, 1.19	$C^\gamma H_2$ 1.79, 1.79
Leu-23	9.19	3.68	0.89, 1.24	$C^\gamma H$ 1.25, $C^{\delta 1,2}H_3$ 0.63, 0.86	Pro-57		4.21	1.81, 1.81	$C^\gamma H_2$ 1.99, 1.99, $C^\gamma H_2$ 3.58, 3.80
Gly-24	8.03	3.37, 4.17			Phe-58	7.64, 7.48	4.58	2.72, 2.42	$C^\delta H_2$ 7.00, 6.75, $C^\epsilon H_2$ 6.93, 6.95, $C^\zeta H$ 6.76
Val-25	7.75	4.41	2.00	$C^{\gamma 1,2}H_3$ 0.58, 0.50					
Tyr-26	7.84, 7.75	4.61	3.27, 2.76	$C^{\gamma 1,2}H$ 7.14, 7.14, $C^{\gamma 1,2}H$ 6.76, 6.76	Pro-59				
					Ser-60	8.22	3.76	4.27, 4.27	
Gln-27	9.15	3.66	2.02, 2.02	$C^\gamma H_2$ 2.23, 2.23, $N^{\gamma 2}H_2$ 7.49, 6.82	Asn-61	8.12	4.60	2.66, 2.66	$N^{\delta 2}H_2$ 7.45, 6.75
					Lys-62	8.07	4.11	1.69, 1.59	
Ser-28	8.51	4.09	3.78, 3.84		Lys-63	8.29	4.25	1.71, 1.61	
Ala-29	7.30	4.15	1.49		Thr-64	8.10	4.28	4.12	$C^{\gamma 2}H_3$ 1.06
Ile-30	7.26	3.60	2.30	$C^{\gamma 2}H_3$ 0.76	Thr-65	7.94	4.22	4.12	$C^{\gamma 2}H_3$ 1.04
Asn-31	7.98	4.19	2.89, 2.66	$N^{\delta 2}H_2$ 6.88, 7.55	Ala-66	7.88	4.00	1.20	
Lys-32	8.08	3.94	1.59, 1.69						

[a] Assignments are reported for a 3 mM sample of cro at 35 °C dissolved in 10 mM potassium phosphate, pH 6.8. Chemical shifts are referenced to internal DSS and are accurate at least to ±0.02 ppm and often to ±0.01 ppm. Resonances underscored were obtained for cro dissolved in 10 mM phosphate, pH 4.8, 0.2 M KCl, and 0.1 mM EDTA and are reported when they differ by more than ±0.05 ppm between the two samples. When no chemical shift is listed for a particular proton, no individual resonance assignment was possible. IUPAC–IUB (1969) nomenclature is followed for identifying side chain atoms. [b] n.o., not observed. [c] The $C^\alpha H_2$ protons of Gly-48 have identical chemical shifts; this was corroborated by two-dimensional double-quantum spectroscopy (data not shown).

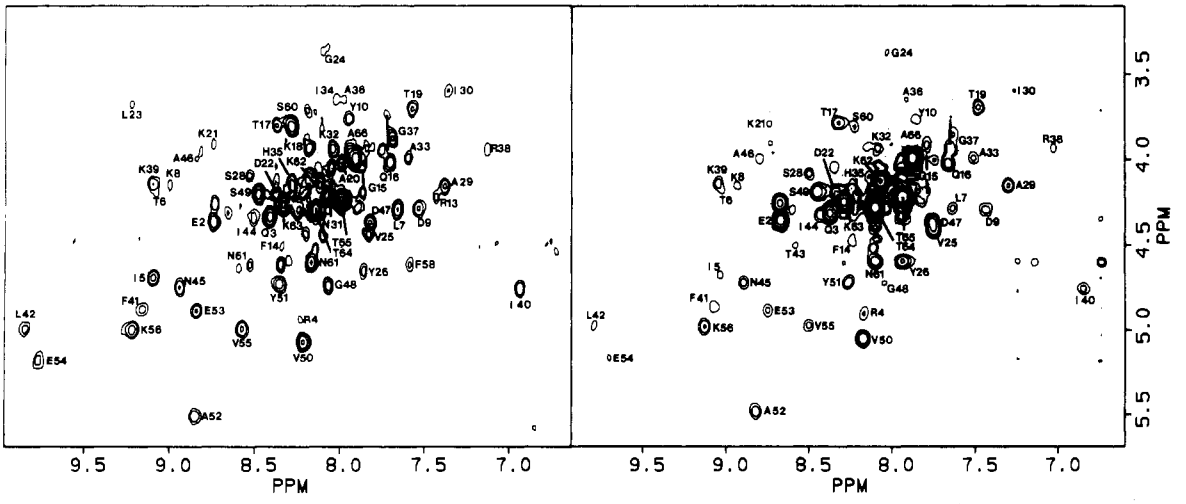

FIGURE 11: COSY "fingerprint" regions for cro repressor in H_2O. Left: Sample dissolved in 10 mM potassium phosphate, pH 4.8, 0.2 M KCl, and 0.1 mM EDTA. Right: Sample dissolved in 10 mM potassium phosphate, pH 6.8. The identity of each cross peak, when known, is labeled. Spectra are plotted at a level slightly above noise; as a result some weaker cross peaks are not visible in these plots. In addition, some artifacts due to the solvent resonance at 4.60 ppm are seen.

structure, but this is not certain. In the sample containing 0.2 M KCl, two cross peaks are identified as Asn-61; both give RELAY cross peaks to the same $C^\beta H$ resonance (data not shown).

Discussion

Sequence-specific resonance assignments of cro repressor are required for critically investigating the interaction of this repressor with its operator sequence. These assignments are now nearly complete. In terms of testing the proposed model for DNA binding by cro (Ohlendorf et al., 1982), the missing assignments of the Lys-32 $C^{\epsilon}H_2$ and $N^{\zeta}H_3$ resonances are unfortunate as these are predicted to be involved in several contacts with the operator major groove. Most other protons predicted to be involved in specific binding have been identified, as well as many of the protons involved in nonspecific binding. In a few cases, backbone resonances were assigned although COSY NH–$C^{\alpha}H$ cross peaks were not clearly observed. Three residues (Ala-11, Met-12, Arg-13) are consecutive, and the absence of their COSY cross peaks is likely to be due to broadening by the same process, whatever it may be.

The C-terminal region has also been postulated to be involved in binding, but this region was disordered and not observed in the crystal structure. This region is a random coil in solution, too, on the basis of three lines of evidence. First, the $^3J_{NH-C^{\alpha}H}$ couplings of these residues (measured in a one-dimensional spectrum) are all near 7 Hz, suggesting that they are averaged by random motion. Second, strong inter- and intraresidue $d_{\alpha N}$ NOEs are seen for residues 62–66, indicative of random coil (Wüthrich et al., 1984). Third, the NH–$C^{\alpha}H$ COSY cross peaks for these residues are all considerably narrower than other peaks in the spectrum, implying that there is additional mobility of this region.

In the crystal structure Pro-59 is a cis proline, but a cis to trans isomerization may be taking place in solution. Four lines of evidence support this hypothesis. First, the resonances for Pro-57 could be found, although they were weak (which is common for prolines). If Pro-59 is undergoing slow isomerization, then splitting of resonances may be enough to weaken the signals to the point where they cannot be observed above noise. Second, the COSY NH–$C^{\alpha}H$ cross peaks for Ser-60 and Asn-61 are split, which could be explained by two forms of Pro-59. Third, Phe-58 is *apparently* flipping at a slow rate, as the $C^{\delta}H,H'$ and $C^{\epsilon}H,H'$ ring protons appear to be inequivalent. An alternative explanation for the splitting would be the existence of two forms of Pro-59. Lastly, if Pro-59 were a cis proline, then the crystal structure predicts that a strong NOE between the Phe-58 and Pro-59 α protons should be seen; this is not the case. Nevertheless, until direct evidence of a cis to trans isomerization is found (namely, assignment of two forms of Pro-59), our conclusions must be labeled tentative.

Some identifications of cro spin systems, especially for the aromatic residues, have been previously published. All of the tyrosine ring resonances were first identified by Kirpichnikov and co-workers (Kirpichnikov et al., 1982; Kurochkin & Kirpichnikov, 1982) using one-dimensional NOE experiments, although no sequence-specific information was determined. Lu, Arndt, and their co-workers (Arndt et al., 1983) later corroborated these results using 3,5-dideuteriotyrosine substitution. Both groups were able to find the ring resonances for Phe-14 (again, without sequence information), although the other two phenylalanine ring spin systems were not correctly identified. Arndt et al. (1983) also attempted to identify the $C^{\alpha}H$ and $C^{\beta}H$ resonances of some of the aromatic residues using one-dimensional NOE experiments; their conclusions are incorrect, as are their attempts to use the crystal structure to interpret their NOEs to derive sequence-specific assignments. Sufficient data were not presented, so that any explanation of the discrepancies between their results and the assignments presented here is not possible.

Using tyrosine fluorescence quenching, Boschelli (1982) suggested that variations in the cro dimer structure occurred between 0.04 and 0.18 M ionic strength. This may not be due to a global structural change, but rather to a change in the local structure at Tyr-26. The amide resonance of Tyr-26 shifts by −0.09 ppm in the 0.2 M KCl sample (the changes in chemical shift of the other Tyr-26 resonances are much less). In addition, an NOE from the amide to the $C^{\delta 1,2}H$ resonance at low ionic strength is not seen after salt addition. The hydroxyl group of Tyr-26 is predicted to be involved in sequence-specific DNA binding (Ohlendorf et al., 1982), and the $C^{\delta 1,2}H$ resonance of Tyr-26 shifts well downfield when DNA is added (Arndt et al., 1983). Hence, as suggested by Boschelli (1982), a potentially important mechanism for cro–DNA recognition may be a structural change due to ionic strength changes of an interacting amino acid, but whether this has an in vivo function has not been demonstrated. Other minor changes were seen in the spectrum for residues that occur in bends or in "hinge" regions.

Finally, the patterns of NOEs observed during the sequential assignments are indicative of the secondary structure of the molecule (Wüthrich et al., 1984). Hence residues Met-1–Ile-5, Lys-39–Ala-46, and Ser-49–Pro-57 are strands of a β-sheet; residues Leu-7–Gly-15, Thr-17–Leu-23, and Ser-28–Gly-37 are α-helices; and the C-terminal residues are random coil. Cross-strand NOEs between the three β-strands allow the positioning of the strands in the sheet; dimer contact NOEs are also seen between the third β-strands of the symmetry-related subunits. This is essentially the same as the crystal structure. Detailed analysis of the three-dimensional structure of cro using distance geometry calculations is presently under way and will be reported in the near future.

Acknowledgments

We thank Dr. Dennis Hare for his technical help in the early stages of this work, as well as his suggestions and encouragement, and Dr. Rachel Klevit for her critical comments and review of the manuscript.

References

Anderson, W. F., Ohlendorf, D. H., Takeda, Y., & Matthews, B. W. (1981) *Nature (London) 290*, 754–758.

Arndt, K. T., Boschelli, F., Cook, J., Takeda, Y., Tecza, E., & Lu, P. (1983) *J. Biol. Chem. 258*, 4177–4183.

Aue, W. P., Bartholdi, E., & Ernst, R. R. (1976) *J. Chem. Phys. 64*, 2229–2246.

Bax, A., & Drobny, G. (1985) *J. Magn. Reson. 61*, 306–320.

Billeter, M., Braun, W., & Wüthrich, K. (1982) *J. Mol. Biol. 155*, 321–346.

Boschelli, F. (1982) *J. Mol. Biol. 162*, 267–282.

Chou, S.-H., Hare, D., Wemmer, D. E., & Reid, B. R. (1983) *Biochemistry 22*, 3037–3041.

Hare, D., Wemmer, D. E., Chou, S.-H., Drobny, G., & Reid, B. R. (1983) *J. Mol. Biol. 171*, 319–336.

Hsiang, M. W., Cole, R. D., Takeda, Y., & Echols, H. (1977) *Nature (London) 270*, 275–277.

Iwahashi, H., Akutsu, H., Kobayashi, Y., Kyogoku, Y., Ono, T., Koga, H., & Horiuchi, T. (1982) *J. Biochem. (Tokyo) 91*, 1213–1221.

Jeener, J., Meier, B. H., Bachmann, P., & Ernst, R. R. (1979) *J. Chem. Phys. 71*, 4546–4553.

Kaptein, R., Zuiderweg, E. R. P., Scheek, R. M., Boelens, R., & van Gunsteren, W. F. (1985) *J. Mol. Biol. 182*, 179–182.

Kirpichnikov, M. P., Kurochkin, A. V., & Skryabin, K. G. (1982) *FEBS Lett. 150*, 407–410.

Klevit, R. E. (1985) *J. Magn. Reson. 62*, 551–555.

Kurochkin, A. V., & Kirpichnikov, M. P. (1982) *FEBS Lett. 150*, 411-415.
Ohlendorf, D. H., Anderson, W. F., Fisher, R. G., Takeda, Y., & Matthews, B. W. (1982) *Nature (London) 298*, 718-723.
Ptashne, M., Jeffrey, A. D., Johnson, A. D., Maurer, R., Meyer, B. J., Pabo, C. O., Roberts, T. M., & Sauer, R. T. (1980) *Cell (Cambridge, Mass.) 19*, 1-11.
Stassinopoulou, C. I., Wagner, G., & Wüthrich, K. (1984) *Eur. J. Biochem. 145*, 423-430.
States, D. J., Haberkorn, R. A., & Ruben, D. J. (1982) *J. Magn. Reson. 48*, 286-292.
Ulrich, E. L., John, E. M. M., Gough, G. R., Brunden, M. J., Gilham, P. T., Westlar, W. M., & Markley, J. L. (1983) *Biochemistry 22*, 4362-4365.
Wagner, G. (1983) *J. Magn. Reson. 55*, 151-156.
Wagner, G., & Wüthrich, K. (1982) *J. Mol. Biol. 155*, 347-366.
Weber, P. L., Drobny, G., & Reid, B. R. (1985) *Biochemistry* (preceding paper in this issue).
Wemmer, D. E., Chou, S.-H., & Reid, B. R. (1984) *J. Mol. Biol. 180*, 41-60.
Wüthrich, K., Wider, G., Wagner, G., & Braun, W. (1982) *J. Mol. Biol. 155*, 311-319.
Zuiderweg, E. R. P., Kaptein, R., & Wüthrich, K. (1983) *Eur. J. Biochem. 137*, 279-292.
Zuiderweg, E. R. P., Billeter, M., Boelens, R., Scheek, R. M., Wüthrich, K., & Kaptein, R. (1984) *FEBS Lett. 174*, 243-247.

Phosphoenolpyruvate-Dependent Phosphotransferase System. ^{1}H NMR Studies on Chemically Modified HPr Proteins†

H. R. Kalbitzer,* H. P. Muss,‡ R. Engelmann,‡ H. H. Kiltz,§ K. Stüber,∥ and W. Hengstenberg‡
Abteilung Molekulare Physik, Max-Planck-Institut für medizinische Forschung, D-6900 Heidelberg, FRG, Max-Planck-Institut für Züchtungsforschung, Egelspfad, D-5000 Köln, FRG, and Abteilung Biologie and Abteilung Chemie, Ruhruniversität Bochum, D-4360 Bochum, FRG

Received November 27, 1984

ABSTRACT: The low-p*K* tyrosyl residue present in the heat-stable proteins (HPr) of all Gram-positive bacteria studied until now has been labeled by tetranitromethane in the HPr of *Bacillus subtilis* and *Streptococcus faecalis*. The nitrotyrosyl derivatives obtained are fully active in the complementation assay. The labeled tyrosyl residues could be identified as Tyr-37 in both proteins. Reinvestigation of the low-p*K* tyrosyl residue in HPr of *Staphylococcus aureus* resulted in the same assignment. In all three proteins an interaction between nitrotyrosine-37 and the active center His-15 could be observed, leading to an increase in the p*K* of His-15 and a change of its chemical shift parameters. The ^{1}H NMR lines of the complete aromatic spin system of HPr of *B. subtilis* could be assigned by the nitration studies. Labeling of Arg-17 in HPr of *S. aureus* and *S. faecalis* by 1,2-cyclohexanedione in the presence of borate ions causes an almost complete inhibition of its enzymatic activity. In the NMR spectrum the labeling of the arginyl residue influences the resonance lines of His-15: two new resonance lines for the C-2 protons of equal intensity are observed, a fact that could be explained by two different conformations in slow exchange. The p*K* value of His-15 was not changed by the labeling, excluding Arg-17 as responsible for the low p*K* of His-15.

HPr[1] is a constitutive protein of the phosphoenolpyruvate-dependent phosphotransferase system (PTS), a carbohydrate transport system found in virtually all anaerobic and facultatively anaerobic bacteria [for a review see, e.g., Hengstenberg (1977), Dills et al. (1980), or Robillard (1982)]. HPr transfers the phosphoryl group from enzyme I to factor III or enzyme II, which finally becomes bound to the transported carbohydrate during the vectorial phosphorylation. Enzyme I, HPr, and factor III carry the phosphoryl group covalently bound to a histidyl residue. NMR studies showed that in the HPr proteins from all microorganisms studied until now (*Staphylococcus aureus*, *Bacillus subtilis*, *Streptococcus faecalis*, *Streptococcus lactis*, *Escherichia coli*) the phosphoryl group is bound at the N-1 of histidyl ring. Because of its low p*K* the histidyl ring is deprotonated at physiological pH before the phosphoryl transfer, and the phosphorylation of the histidyl ring leads to an unusually large increase in p*K* resulting in a complete protonation of the phosphohistidyl residue (Gassner et al., 1977; Dooijewaard et al., 1979; Kalbitzer et al., 1982). The phosphoryl group is bound to His-15 in HPr of *S. aureus*; the similarity of p*K* values and chemical shifts of the active center histidines suggests a similarity of the overall structure around these histidines (Kalbitzer et al., 1982). The heat-stable proteins of all studied microorganisms except that of *E. coli* contain a tyrosyl residue with a low p*K* value whose chemical shift values are again very similar (Maurer et al., 1977; Kalbitzer et al., 1982). The tyrosyl residue is accessible by tetranitromethane in HPr of *S. aureus*, its nitration re-

† H.P.M. and W.H. were supported by the Deutsche Forschungsgemeinschaft.
* Address correspondence to this author at the Max-Planck-Institut für medizinische Forschung.
‡ Abteilung Biologie, Ruhruniversität Bochum.
§ Abteilung Chemie, Ruhruniversität Bochum.
∥ Max-Planck-Institut für Züchtungsforschung.

[1] Abbreviations: HPr, heat-stable protein(s); PTS, phosphoenolpyruvate-dependent phosphotransferase system; NMR, nuclear magnetic resonance; *E. coli*, *Escherichia coli*; *S. aureus*, *Staphylococcus aureus*; *S. faecalis*, *Streptococcus faecalis*; *S. lactis*, *Streptococcus lactis*; *B. subtilis*, *Bacillus subtilis*; TFA, trifluoroacetic acid; HPTLC, high-performance thin-layer chromatography; Tris-HCl, tris(hydroxymethyl)-aminomethane hydrochloride.

0006-2960/85/0424-4562$01.50/0